Quasi-periodicity and bifurcation phenomena in Ising spin neural networks with asymmetric interactions

1994 J. Phys. A: Math. Gen. 27 8011

(http://iopscience.iop.org/0305-4470/27/24/013)

J. Phys. A: Math. Gen. 27 (1994) 8011–8028. Printed in the UK

Quasi-periodicity and bifurcation phenomena in Ising spin neural networks with asymmetric interactions

S N Laughton and A C C Coolen

Department of Physics—Theoretical Physics, University of Oxford, 1 Keble Road, Oxford OX1 3NP, UK

Received 31 August 1994

Abstract. The evolution of macroscopic order parameters in separable, stochastic neural networks, which becomes deterministic in the thermodynamic limit, can be completely described by the inverse 'temperature' β, the embedding matrix $\mathbf{A}$, and the set of initial conditions $\{m_0\}$. Using mainly the techniques of bifurcation theory we present evidence that the qualitative behaviour is governed by one relevant eigenvalue of the matrix $\mathbf{A}$. We show that a variety of bifurcation phenomena can occur as β is varied, including quasi-periodic solutions displaying mode locking in the disrete time case. We illustrate our results with numerical simulations of, for reasons of computational intensity, the discrete time case only.

1. Introduction

The study of Ising spin models of large recurrent neural networks is essentially split into two sub-disciplines: the study of their static properties and the study of their dynamics. For cases in which the neuronal interactions are symmetric the system will approach an equilibrium state in which detailed balance holds. In this case equilibrium statistical-mechanical techniques can be used and the properties of the system in equilibrium can be derived from the free energy. For cases in which detailed balance does not hold, equilibrium statistical mechanics cannot be used, and the only route available is to study the dynamics. Obviously, analysis of the dynamics at the microscopic level, i.e. the states of individual neurons, is impossible due to the large number of them. Instead we apply a stochastic microscopic dynamics, and derive deterministic equations for macroscopic variables [1–5]. This paper is devoted to the study of these deterministic macroscopic equations. For asymmetric interactions (i.e. systems without detailed balance) we expect complex behaviour, with long period cycles or perhaps even chaotic trajectories. We illustrate typical behaviour with specific examples, and show that the complex behaviour which a network exhibits can be understood qualitatively using bifurcation theory, which can be used to reduce a complex high-dimensional system to a low-dimensional set of equations containing only essential terms from which generic behaviour can be deduced.

Much work has already been done on the complex behaviour of the dynamics of neural networks, and it has been shown that chaotic behaviour is possible in systems with continuous (Langevin-type) neurons [6–13]. Complex behaviour has also been found in systems with discrete-valued neurons [14, 15], though chaos is not possible due to the finite number of microscopic configurations of the system. In all these studies, however, the description is at the microscopic level of individual neurons. In contrast, our study aims

0305-4470/94/248011+18$19.50

at identifying and studying complexity at the deterministic and low-dimensional level of order-parameter evolution.

In the limit of high noise the only stable fixed point is the origin, representing a paramagnetic macroscopic state. As the noise is varied, the form of bifurcation from this fixed point depends solely on one relevant eigenvalue of the embedding matrix which determines the neuronal interactions.

The model to be studied consists of N binary-valued neurons (Ising spins) $s_i(t)$, coupled by interactions $J_{ij} = (1/N)\sum_{\mu,\nu=1}^{p} \xi_i^\mu A_{\mu\nu}\xi_j^\nu$. The spins can be updated asynchronously or synchronously, and evolve due to a stochastic local-field alignment which we define by a continuous-time master equation, or a discrete-time Markov process, respectively. In the case of the asynchronous, continuous-time process transition rates are given by $w_i(F_i s \to s) = \frac{1}{2}(1 - s_i \tanh \beta h_i(s))$. Similarly the transition probability for the synchronous, discrete-time process is given by $w_i(F_i s \to s) = \frac{1}{2}(1 + s_i \tanh \beta h_i(s))$. These are chosen to lead to Gibb's and Peretto's [16] probability distributions, respectively, in equilibrium. The local fields are given by $h_i(s) = \sum_{j\neq i} J_{ij}s_j$, and β plays the part of the inverse temperature in a spin system, parametrizing the noise. Here F_i is the spin-flip operator $F_i\Phi(s_1, \ldots, s_i, \ldots, s_N) = \Phi(s_1, \ldots, -s_i, \ldots, s_N)$. From these microscopic rules a set of deterministic coupled nonlinear equations for the evolution of the macroscopic overlaps $m^\mu = (1/N)\sum_{i=1}^{N} \xi_i^\mu s_i(t)$ $\mu \in \{1, \ldots, p\}$, strictly valid only in the thermodynamic limit ($N \to \infty$) with $p \ll \sqrt{N}$, can be derived for both asynchronous updating [1, 2] and synchronous updating [3] of neurons, respectively,

$$\frac{\mathrm{d}}{\mathrm{d}t}m^\mu = \left\langle \xi^\mu \tanh\left(\beta \sum_{\eta,\nu=1}^{p} \xi^\eta A_{\eta\nu} m^\nu\right)\right\rangle - m^\mu \tag{1}$$

$$m_{t+1}^\mu = \left\langle \xi^\mu \tanh\left(\beta \sum_{\eta,\nu=1}^{p} \xi^\eta A_{\eta\nu} m_t^\nu\right)\right\rangle. \tag{2}$$

Here the angular brackets $\langle\ \rangle$ denote an average over the p unbiased random variables $\xi^\mu \in \{-1, 1\}$. For neural networks we interpret ξ_i^μ as bits of patterns or sequences stored by the network. We study (1) and (2) purely as a mathematical exercise, without reference to their interpretation regarding neural networks, although retaining the terminology associated with them, only returning to any physical interpretation of the results at the end.

Recently, Lyapunov functions have been found for (1) and (2) for the case where the embedding matrix $\mathbf{A}$ is symmetric [17], guaranteeing approach to equilibrium. For asymmetric $\mathbf{A}$, however, exact results are usually impossible to obtain and we must resort to the qualitative techniques of bifurcation theory to study how the system deviates from the trivial fixed point, and numerical iteration of the dynamical equations. For a review of the methods of bifurcation theory see [18, 19]. We classify the bifurcations as steady state, or Hopf depending on the form of the relevant eigenvalue (α) of the linearized equations, and observe that in the latter case quasi-periodic behaviour is observed including mode-locked regions (a common feature of nonlinear dynamics). The mode-locked regions are known as Arnold tongues [20, 21] and appear when the system locks into a certain cycle for a range of parameter values. They are related to resonances of the eigenvalue α.

2. Bifurcation analysis

In the following sections we carry out a bifurcation theory analysis for (1) and (2). We show that to cubic order centre-manifold reduction does not alter the expansion of the

dynamic equations, hence we need only carry out the reduction to normal form for the cases $p = 1$ and 2, since these will lead to the interesting and well understood *steady state* and *Hopf* bifucrcations, respectively. All other cases without further degeneracy in the critical eigenvalues will therefore, to low orders at least, behave in a similar manner.

2.1. Linear analysis and centre-manifold reduction

The first step to analysing the dynamics is to linearize the equations of motion (1) and (2) about the trivial fixed point $m = 0$.

$$\frac{\mathrm{d}m}{\mathrm{d}t} = \beta \mathbf{A} m - m + \mathcal{O}(m^3) \qquad m_{t+1} = \beta \mathbf{A} m_t + \mathcal{O}(m^3). \tag{3}$$

A bifurcation from the trivial fixed point occurs when there is a loss of linear stability, this occurs as $\beta \to \beta_c + \delta\beta$, where $\delta\beta$ is an infinitesimal increment, and β_c is given by

$$\beta_c = \frac{1}{\max \mathrm{Re}(\alpha(\mathbf{A}))} \qquad \beta_c = \frac{1}{\max |\alpha(\mathbf{A})|} \tag{4}$$

for the continuous-time and discrete-time cases, respectively (where $\alpha(\mathbf{A})$ *are the* eigenvalues of the matrix $\mathbf{A}$). Note that due to the Hartman–Grobman theorem [22], these results give strong bounds on the region where the only long-time solution is the trivial fixed point, however, these are only true locally, i.e. when the solution is already close to the origin. Bounds for the global stability of the trivial fixed point will be derived in the next section.

We can now classify the bifurcations according to the forms of the eigenvalues α. Bifurcations where the relevant eigenvalue α is a real number are known as *steady-state* bifurcations. Bifurcations with a complex conjugate pair of eigenvalues are known as *Hopf* bifurcations. There is a further special case relevant to the discrete-time case only when the relevant eigenvalue is a negative number these are known as *pitchfork* or *period-doubling* bifurcations.

We consider first the expansion of the dynamic equations (1) and (2)

$$\left.\begin{matrix} \dfrac{\mathrm{d}m^\nu}{\mathrm{d}t} + m^\nu \\ m^\nu_{t+1} \end{matrix}\right\} = \langle \xi^\nu \tanh \beta \xi \mathbf{A} m_t \rangle$$

$$\simeq \beta \mathbf{A} m_t \left\{ 1 - \tfrac{1}{3}\beta^2 \left[3\left(m_t \mathbf{A}^\dagger \mathbf{A} m_t \right) - 2\left((\mathbf{A} m_t)^\nu \right)^2 \right] \right\} + \mathcal{O}(m^5). \tag{5}$$

Now consider a matrix $\mathbf{T}$ such that $\mathbf{T}^{-1}\mathbf{A}\mathbf{T}$ has the block diagonal form $\begin{pmatrix} \mathbf{A}_1 & 0 \\ 0 & \mathbf{A}_2 \end{pmatrix}$, where $\beta\mathbf{A}_1$ has only critical eigenvalues—i.e. with real parts equal to one in the continuous-time case, and modulus equal to one in the discrete-time case. We label the number of critical eigenvalues n_c. We also re-label the coordinate $(\mathbf{T}^{-1} m_t)^\nu = y_t^\nu$ if $\nu \leqslant n_c$ and $(\mathbf{T}^{-1} m_t)^\nu = z_t^\nu$ if $\nu > n_c$. Substituting $z = h(y)$ into (5) can then be used to define the centre manifold. We propose a power-series expansion $h(y) = \sum_{\mu\nu} \phi_{\mu\nu} y^\nu y^\mu + \sum_{\mu\nu\lambda} \Theta_{\mu\nu\lambda} y^\nu y^\mu y^\lambda + \mathcal{O}(y^4)$, where the constant and linear terms are missing due to the boundary conditions $h(0) = 0$ and $D_y h(0) = 0$. By comparing terms in y^n we obtain a set of simultaneous equations determining the expansion coefficients ϕ, Θ etc. Because the lowest-order terms in $h(y)$ are of order y^2 we can see that to order y^3 the equations of motion on the centre manifold are simply given by

$$\left.\begin{matrix} \dfrac{\mathrm{d}y^\nu}{\mathrm{d}t} + y^\nu \\ y^\nu_{t+1} \end{matrix}\right\} = \beta (A_1)_{\nu\mu} y_t^\mu \left\{ 1 - \beta^2 y_t \mathbf{A}_1^\dagger \mathbf{A}_1 y_t \right\} + \tfrac{2}{3}\beta^3 T^{-1}_{\nu\eta} \left(T_{\eta\lambda} \left(\sum_{\rho \leqslant n_c} (A_1)_{\lambda\rho} y_t^\rho \right) \right)^3 + \mathcal{O}(y^4) \tag{6}$$

i.e. to cubic order the forms of the equations of motion on the centre manifold are the same form as the full equations of motion. Therefore we carry out all the following stages of analysis for the $p = 1$ and 2 cases only, since the equations of motion for $p > 2$ displaying steady state and Hopf bifurcations, respectively, will be the same form as these, with slightly different numerical constants up to cubic order.

2.2. *Normal forms for one and two patterns*

For a network trained with one pattern, the embedding matrix $\mathbf{A}$ is simply a number and hence symmmetric, the Lyapunov functions [17] therefore apply, and approach to equilibrium is guaranteed. We can investigate the behaviour, however, using bifurcation theory to discover how the fixed point deviates from the trivial fixed point. This will also serve as a useful introduction to the methods which will be applied to networks with more patterns. First the equations of motion are expanded in powers of m:

$$\frac{\mathrm{d}m}{\mathrm{d}t} \simeq (\beta A - 1)m - \tfrac{1}{3}(\beta A m)^3 + \cdots \qquad m_{t+1} \simeq \beta A m_t - \tfrac{1}{3}(\beta A m_t)^3 + \cdots . \tag{7}$$

We can see that there will be a steady-state bifurcation when $\beta = \beta_c = 1/A$ for the continuous-time case, and $\beta = \beta_c = 1/|A|$ for the discrete-time case. Since the equations are one dimensional, we do not have to perform the centre-manifold reduction, and can at once move on to the normal-form reduction. In order to remove nonlinear terms of order-k we apply the nonlinear coordinate changes $m = m' + \phi^k(m') = m' + a_k^k m^k$. The essential terms to be retained are those in the kernel of a particular operator $L(\phi^k(m))$, $\tilde{L}(\phi^k(m))$ for continuous and discrete time, respectively [18].

In our case the equations for $L\big(\phi^k(m)\big)$, $\tilde{L}\big(\phi^k(m)\big)$ $\big(\phi^k(m) = a_k^k m^k\big)$ are

$$L\big(\phi^k(m)\big) = (\beta A - 1)a_k^k(1-k)m^k \qquad \tilde{L}\big(\phi^k(m)\big) = \beta A a_k^k m^k\big(1 - (\beta A)^{k-1}\big). \tag{8}$$

We can see that $L\big(\phi^k(m)\big) = 0$ requires $k = 1$ or $\beta A = 1$, and $\tilde{L}(\phi^k(m)) = 0$ requires $|\beta A| = 1$, which are exactly the conditions satisfied at criticality. Hence no nonlinear terms can be removed. Therefore, to proceed further we expand the equations of motion $(\mathrm{d}m/\mathrm{d}t, m_{t+1} - m_t = V(\beta, m))$ about the critical point $q = 0$, $\beta_c = 1/A$, or $\beta_c = 1/|A|$ for the discrete-time case giving the normal forms for $A > 0$

$$\left.\begin{matrix} \dfrac{\mathrm{d}m}{\mathrm{d}t} \\ m_{t+1} - m_t \end{matrix}\right\} \simeq m_t\left(\left(\frac{\beta}{\beta_c} - 1\right) - \tfrac{1}{3}m_t^2\right). \tag{9}$$

Normal forms such as these give rise to pitchfork bifurcations. We can see that fixed points of the motion are $m_t = 0$ and $m_t = \pm\sqrt{3(\beta/\beta_c - 1)}$, and that $m_t = 0$ is stable for $\beta/\beta_c < 1$, and $m_t = \pm\sqrt{3(\beta/\beta_c - 1)}$ is stable for $\beta/\beta_c > 1$.

Interesting things happen when $A < 0$ in the discrete-time case, since then $\beta_c = \mathrm{sgn}A/A$ so the normal form is

$$m_{t+1} - m_t \simeq m_t\left(\mathrm{sgn}\,A\left(\frac{\beta}{\beta_c} - 1\right) - \tfrac{1}{3}m_t^2\right) \tag{10}$$

hence for $A < 0$ the system will settle into a two-cycle—oscillating between the two stable fixed points. For this reason a *pitchfork* bifurcation is often known as a *period-doubling* bifurcation. An infinite cascade of period-doubling bifurcations as succesive iterates of the quadratic map lose stability is responsible for the transition to chaos investigated in [23, 24]. This, however, will not occur in this system since the two-cycle is always stable above the critical point.

The analysis for networks trained with more than one pattern displaying steady-state bifurcations can easily be carried out since the centre-manifold reduction showed that, to cubic order, the form of equations is not altered. This is of course dependent on the relevant eigenvalue of the matrix **A** (the one with the largest modulus) being a real number. If the relevant eigenvalue is a complex conjugate pair, the normal form is two-dimensional, and the system will display a Hopf bifurcation.

For networks trained with only two patterns there are four free parameters in the embedding matrix making it a relatively simple case to analyse. Steady-state bifurcations will occur when the relevant eigenvalue is pure real and Hopf bifurcations when the eigenvalue is a complex conjugate pair.

For cases where the relevant eigenvalues form a complex conjugate pair at criticality, the system undergoes a Hopf bifurcation. In this case the behaviour is slightly different for the continuous-time case and the discrete-time case. In the discrete-time case if the eigenvalues exhibit resonance, i.e. if there exists n such that $\alpha_c^n = 1$, then terms are introduced into the normal form which cause effects such as mode locking. Nonlinear effects cause the system to lock into one frequency over a range of the external driving frequency. It can be understood in resonant sytems since if m exists then the dynamics are effectively undergoing a steady-state bifurcation in $m_{t+n} = F(m_t)$, hence the system will display a period-n cycle. As other parameters are varied the system can pass through several resonances, causing the devil's staircase structure.

Consider a matrix $\mathbf{A} = \begin{pmatrix} 1 & \alpha \\ -\alpha & 1 \end{pmatrix}$. This has conjugate eigenvalues $1 \pm \mathrm{i}\alpha$ and there will be a Hopf bifurcation at $\beta_c = 1$ in the continuous-time case, and $\beta_c = 1/\sqrt{\alpha^2+1}$ in the discrete-time case. We proceed with the bifurcation analysis by expanding the dynamical equations (1) and (2), keeping only the first nonlinear term since higher-order terms will be negligible at the critical point, and since we can always consider higher-order terms later as perturbations. We now define a matrix **U** which diagonalizes **A**, and define new variables x, so that (5) for this matrix becomes

$$\left.\begin{matrix} x_{t+1} \\ \dfrac{\mathrm{d}x}{\mathrm{d}t} + x \end{matrix}\right\} = \beta \begin{pmatrix} 1+\mathrm{i}\alpha & 0 \\ 0 & 1-\mathrm{i}\alpha \end{pmatrix} \begin{pmatrix} x_1 \\ x_2 \end{pmatrix}$$
$$+\tfrac{1}{6}\beta^3 x_1^3 \begin{pmatrix} (-1-7\mathrm{i})\alpha^3 + (-9+3\mathrm{i})\alpha^2 + (3-3\mathrm{i})\alpha + (-5-\mathrm{i}) \\ (1+\mathrm{i})\alpha^3 + (3-3\mathrm{i})\alpha^2 + (-3-3\mathrm{i})\alpha + (-1+\mathrm{i}) \end{pmatrix}$$
$$+\tfrac{1}{6}\beta^3 x_1^2 x_2 \begin{pmatrix} (-3+3\mathrm{i})\alpha^3 + (3+3\mathrm{i})\alpha^2 + (-3+3\mathrm{i})\alpha + (3+3\mathrm{i}) \\ (-3+9\mathrm{i})\alpha^3 + (-3+3\mathrm{i})\alpha^2 + (-3+9\mathrm{i})\alpha + (-3+3\mathrm{i}) \end{pmatrix}$$
$$+\tfrac{1}{6}\beta^3 x_1 x_2^2 \begin{pmatrix} (-3-9\mathrm{i})\alpha^3 + (-3-3\mathrm{i})\alpha^2 + (-3-9\mathrm{i})\alpha + (-3-3\mathrm{i}) \\ (3+3\mathrm{i})\alpha^3 + (-3+3\mathrm{i})\alpha^2 + (3+3\mathrm{i})\alpha + (-3+3\mathrm{i}) \end{pmatrix}$$
$$+\tfrac{1}{6}\beta^3 x_2^3 \begin{pmatrix} (-1+\mathrm{i})\alpha^3 + (-3-3\mathrm{i})\alpha^2 + (3-3\mathrm{i})\alpha + (1+\mathrm{i}) \\ (-1+7\mathrm{i})\alpha^3 + (-9-3\mathrm{i})\alpha^2 + (3+3\mathrm{i})\alpha + (-5+\mathrm{i}) \end{pmatrix}$$
$$+\mathcal{O}(x^5). \tag{11}$$

We now apply coordinate changes $x \to x + \phi(x)$ to reduce the equations to normal form. In order to find the non-removable terms we need to find the zero eigenvalues of $L(\phi^k(m))$, $\tilde{L}(\phi^k(m))$. First, transforming coordinates $\phi^k(x) = \mathbf{U}^\dagger \phi^k(m)$ then

$$L(\phi^k(x)) = \begin{pmatrix} \lambda_+ & 0 \\ 0 & \lambda_- \end{pmatrix} \begin{pmatrix} \phi_1^k(x) \\ \phi_2^k(x) \end{pmatrix} - \begin{pmatrix} \partial\phi_1^k(x)/\partial x_1 & \partial\phi_1^k(x)/\partial x_2 \\ \partial\phi_2^k(x)/\partial x_1 & \partial\phi_2^k(x)/\partial x_2 \end{pmatrix} \begin{pmatrix} \lambda_+ x_1 \\ \lambda_- x_2 \end{pmatrix} \tag{12}$$

$$\tilde{L}(\phi^k(x)) = \begin{pmatrix} \lambda_+ & 0 \\ 0 & \lambda_- \end{pmatrix} \begin{pmatrix} \phi_1^k(x_1, x_2) \\ \phi_2^k(x_1, x_2) \end{pmatrix} - \begin{pmatrix} \phi_1^k(\lambda_+ x_1, \lambda_- x_2) \\ \phi_2^k(\lambda_+ x_1, \lambda_- x_2) \end{pmatrix}. \tag{13}$$

We can see that suitable basis vectors are $\xi_+^{k,l}(x_1,x_2)=\binom{x_1^l x_2^{k-l}}{0}$, $\xi_-^{k,l}(x_1,x_2)=\binom{0}{x_1^l x_2^{k-l}}$, $l=0,1,2,\ldots,k$ and that the corresponding eigenvalues of $L(\phi(x))$, $\tilde{L}(\phi(x))$, with $\lambda_\pm=\gamma\pm i\omega$ for the continuous-time case and $\lambda_\pm=ae^{\pm i2\pi\psi b}$ for the discrete-time case are

$$\alpha_\pm^{k,l}=(1-k)\gamma+i\omega(k-2l\pm1)\qquad \tilde{\alpha}_\pm^{k,l}=ae^{\pm i2\pi\psi b}\left(1-a^{k-1}e^{-i2\pi\psi b(k-2l\pm1)}\right). \tag{14}$$

At the critical point $\gamma=0$ and $a=b=1$. Zero eigenvalues in the continuous-time case therefore require $k=2l\pm1$, i.e. k must be odd. Therefore the eigenvectors for the irreducible part of the equations of motion are $\xi_+^k(x)=\binom{x_1|x_1\,x_2|^{(k-1)/2}}{0}$ and $\xi_-^k(x)=\binom{0}{x_2|x_1\,x_2|^{(k-1)/2}}$ with $k=3,5,\ldots$. Therefore the normal form is

$$\begin{pmatrix}\dot{x}_1\\ \dot{x}_2\end{pmatrix}=\begin{pmatrix}\gamma+i\omega & 0\\ 0 & \gamma-i\omega\end{pmatrix}\begin{pmatrix}x_1\\ x_2\end{pmatrix}+\sum_{j=1}^{\infty}|x_1\,x_2|^j\begin{pmatrix}a_jx_1\\ \bar{a}_jx_2\end{pmatrix} \tag{15}$$

where a_j, $\bar{a}_j$ are the coefficients in the equations of motion. If we write $x_{1,2}=re^{\mp i\theta}$ then $\dot{x}_{1,2}/x_{1,2}=\dot{r}/r\mp i\dot{\theta}$ so in polar coordinates the equations of motion become

$$\dot{r}=r\left(\gamma+\sum_{j=1}^{\infty}\mathrm{Re}(a_j)r^{2j}\right)\qquad \dot{\theta}=-\omega-\sum_{j=1}^{\infty}\mathrm{Im}(a_j)r^{2j}. \tag{16}$$

In our case $\gamma=\beta-1$, $\omega=\alpha\beta$ and $a_1=\frac{1}{2}\beta^3(\alpha^2+1)((1-\alpha)+i(1+\alpha))$, so our equations of motion close to the critical point $\beta_c=1$ are

$$\begin{aligned}\dot{r}&=\left(\frac{\beta}{\beta_c}-1\right)r+\tfrac{1}{2}\beta^3(\alpha^2+1)(1-\alpha)r^3+\mathcal{O}(r^5)\\ \dot{\theta}&=-\alpha\beta-\tfrac{1}{2}\beta^3(\alpha^2+1)(1+\alpha)r^2+\mathcal{O}(r^4).\end{aligned} \tag{17}$$

Notice that both equations are independent of θ. Close to the critical point where higher-order terms can be omitted, the system will settle into a cycle of fixed radius (the Hopf radius), for $\alpha>1$ this is given by $r_H=\sqrt{2(\beta/\beta_c-1)/(\beta^3(\alpha^2+1)(\alpha-1))}$, with angular velocity approximately $\dot{\theta}=-\alpha\beta-(\beta/\beta_c-1)(1+\alpha)/(1-\alpha)$. For $\alpha<1$ higher-order terms are needed to determine the Hopf radius.

In the discrete-time case things are a little more complicated, since the conditions for zero eigenvalues are that $\psi(k-2l\pm1)=m$, where m is an integer. If ψ is irrational this can only occur for $k-2l\pm1=0$, however, if ψ is rational $=p/m$ then we also have solutions $k-2l\pm1=nq$. If this is satisfied for some value s of m then the basis vectors for removing the sth terms are $\xi_+^s=\binom{x_2^{s-1}}{0}$ $\xi_-^s=\binom{0}{x_1^{s-1}}$ therefore the normal form is

$$\begin{pmatrix}x_1(t+1)\\ x_2(t+1)\end{pmatrix}=\begin{pmatrix}ae^{i2\pi\psi b} & 0\\ 0 & ae^{-i2\pi\psi b}\end{pmatrix}\begin{pmatrix}x_1\\ x_2\end{pmatrix}+\sum_{j=1}^{\infty}|x_1\,x_2|^j\begin{pmatrix}a_jx_1\\ \bar{a}_jx_2\end{pmatrix}+\sum_{k=2}^{\infty}\begin{pmatrix}a_k^*x_2^k\\ \bar{a}_k^*x_1^k\end{pmatrix} \tag{18}$$

where a_j, $\bar{a}_j$, a_k^* and $\bar{a}_k^*$ are the coefficients for the non-resonant, and resonant terms, respectively. In terms of polar coordinates the equations of motion are

$$r_{t+1}=r_t\left|a+\sum_{j=1}^{\infty}a_jr_t^{2j}+\sum_{k=3}^{\infty}a_k^*r_t^{k-1}e^{ik\theta_t}\right| \tag{19}$$

$$\theta_{t+1}-\theta_t=-2\pi\psi b-\arg\left(a+\sum_{j=1}^{\infty}a_je^{-i2\pi\psi b}r_t^{2j}+\sum_{k=2}^{\infty}a_k^*r_t^ke^{-i(k+1)\theta_t}\right). \tag{20}$$

For our case $a=\beta\sqrt{\alpha^2+1}$, $2\pi\psi b=\tan^{-1}(\alpha)$, $a_1=\frac{1}{2}\beta^3(\alpha^2+1)((1-\alpha)+i(1+\alpha))$ giving equations of motion close to the critical point $\beta_c=1/\sqrt{\alpha^2+1}$ in the absence of

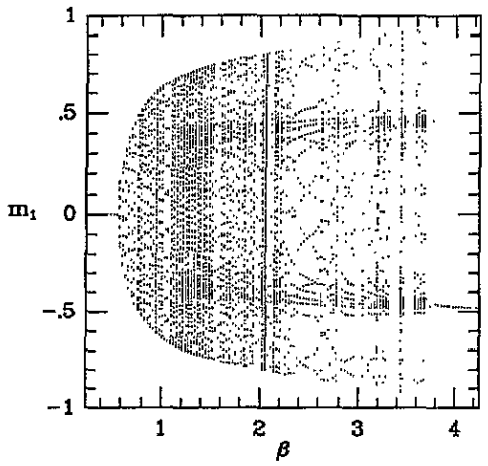

Figure 1. Hopf bifurcation diagram as a function of β for $p = 3$.

strong resonances

$$r_{t+1} = r_t \left| \frac{\beta}{\beta_c} - \tfrac{1}{2}\beta^3(\alpha^2+1)((1-\alpha)+\mathrm{i}(\alpha+1))r_t^2 + \mathcal{O}(r^4) \right| \tag{21}$$

$$\theta_{t+1} - \theta_t = -\tan^{-1}(\alpha) - \arg\left(1 + \tfrac{1}{2}\beta^2(\alpha^2+1)((1-\alpha)+\mathrm{i}(\alpha+1))\mathrm{e}^{-\mathrm{i}\tan^{-1}(\alpha)}r_t^2 + \mathcal{O}(r^4)\right). \tag{22}$$

This predicts a steady-state Hopf radius, close to the critical point where higher-order terms can be neglected given by $r_t^2 = (-(\alpha-1) \pm \sqrt{2/\beta^2 - (\alpha+1)^2})/(\alpha^2+1)^{3/2}$.

Figure 1 shows a bifurcation diagram for the matrix

$$\mathbf{A} = \begin{pmatrix} 1 & 1 & -1 \\ 1 & 1 & 0 \\ 0 & 1 & 1 \end{pmatrix} \qquad \alpha = \begin{cases} 0.324\,718 \\ 1.662\,36 + 0.562\,28\mathrm{i} \\ 1.662\,36 - 0.562\,28\mathrm{i} \end{cases} \qquad |\alpha| = \begin{cases} 0.324\,718 \\ 1.754\,88 \\ 1.754\,88\,. \end{cases} \tag{23}$$

Here we expect to see a Hopf bifurcation to quasi-periodic behaviour at $\beta = 1/1.754\,88 = 0.569\,84$.

In figure 1 we clearly see the bifurcation from trivial fixed point to quasi-periodic behaviour, for a network with the embedding matrix (23). The period is obviously dependent on β, as illustrated by the variation in density of points, and the periodic windows are clearly visible. This behaviour is described by (21) and (22).

The existence of resonances will cause nonlinear θ_t terms in the arg term, causing phenomena such as mode locking, and could lead to a transition to chaos, if the θ_t map loses invertibility. These equations are strictly only valid in a small interval around the critical point. As we move away from the critical point, the resonances, inititially points on the unit circle will grow giving Arnold tongues [20]. It is this effect which produces mode locking.

3. Exact results

Analytical results for (1) and (2) are difficult, if not impossible, to obtain due to the nonlinearity of the mapping and the lack of symmetries in the matrix **A**. Some results have been found for specific choices of the matrix **A** [17, 25]. It is possible, however, to

derive some bounds on β and the matrix $\mathbf{A}$, for which we can predict the behaviour. For $p = 1$ or 2 some exact results, valid for all β and $\mathbf{A}$, can be found.

3.1. Bounds for low and high β

It is clear from (1) and (2) that in the limit $\beta \to 0$, the network will always settle into the trivial fixed point $m = 0$. We wish to derive some rigorous bounds for β, dependent on the properties of the matrix $\mathbf{A}$, such that the network will always settle into the trivial fixed point.

Consider two vectors m and k related by the relation $m = \langle \xi \tanh(\beta \xi k) \rangle_\xi$. Since tanh is an odd function and the ξ's are independent, unbiased random variables with values ± 1, we can write

$$m^\mu = \left\langle \tanh\left(\beta k^\mu + \beta \sum_{\rho \neq \mu} \xi^\rho k^\rho\right)\right\rangle. \tag{24}$$

Now $\partial m^\mu / \partial k^\mu \geqslant 0$, and if $k^\mu = 0$ then $m^\mu = 0$ (the ξ's are randomly distributed over $\{-1, +1\}$). From this we can see that $\operatorname{sgn}[m^\mu] = \operatorname{sgn}[k^\mu]$ and $|m^\mu| = \langle \tanh(\beta |k^\mu| + \beta \sum_{\rho \neq \mu} \xi^\rho k^\rho) \rangle$ Since the ξ's are randomly ± 1, we can replace ξ in any expression with $-\xi$. Therefore

$$|m^\mu| = \tfrac{1}{2}\left\langle \tanh \beta |k^\mu| + \beta \sum_{\rho \neq \mu} \xi^\rho k^\rho \right\rangle + \tfrac{1}{2}\left\langle \tanh \beta |k^\mu| - \beta \sum_{\rho \neq \mu} \xi^\rho k^\rho \right\rangle. \tag{25}$$

This is a function of the general form $f(|x| + y) + f(|x| - y)$, which equals $f(|x| + |y|) + f(|x| - |y|)$. Therefore

$$|m^\mu| = \tanh \beta |k^\mu| + \left\langle \int_0^1 \mathrm{d}\lambda\, \beta \left| \sum_{\rho \neq \mu} \xi^\rho k^\rho \right| \left\{ \tanh^2\left(\beta |k^\mu| - \beta\lambda \left| \sum_{\rho \neq \mu} \xi^\rho k^\rho \right|\right) - \tanh^2\left(\beta |k^\mu| + \beta\lambda \left| \sum_{\rho \neq \mu} \xi^\rho k^\rho \right|\right)\right\}\right\rangle \tag{26}$$

the second term is always positive, hence $|m^\mu| \leqslant \tanh(\beta |k^\mu|) \leqslant \beta |k^\mu|$ and $m^2 \leqslant \beta^2 k^2$.

Now if we let $k \to \mathbf{A}m$, and $m \to \mathrm{d}m/\mathrm{d}t + m$, where m solves the continuous-time dynamics (1) then we have

$$\left(m + \frac{\mathrm{d}m}{\mathrm{d}t}\right)^2 = m^2 + \frac{\mathrm{d}m^2}{\mathrm{d}t} + \left(\frac{\mathrm{d}m}{\mathrm{d}t}\right)^2 \leqslant \beta^2 m \mathbf{A}^\dagger \mathbf{A} m\,. \tag{27}$$

Hence for $\beta^2 < 1/\alpha_{\max}(\mathbf{A}^\dagger \mathbf{A})$ then $\mathrm{d}m^2/\mathrm{d}t < 0$ and as a result $\lim_{t \to \infty} m = 0$ (where $\alpha_{\max}(\mathbf{A}^\dagger \mathbf{A})$ is the largest eigenvalue of $\mathbf{A}^\dagger \mathbf{A}$).

Similarly in the discrete-time case (2) we choose $m = m_{t+1}$ and $k = \mathbf{A}m_t$, so

$$\frac{m_{t+1}^2}{m_t^2} \leqslant \beta^2 \frac{m_t (\mathbf{A}^\dagger \mathbf{A}) m_t}{m_t^2} \qquad \forall m_t\,. \tag{28}$$

Therefore for $\beta^2 < 1/\alpha_{\max}(\mathbf{A}^\dagger \mathbf{A})$ then $m_{t+1}^2 / m_t^2 < 1$ hence $\lim_{t \to \infty} m_t = 0$.

Notice these are weaker bounds than the ones given by considering the linearization of the equations of motion. They are, however, global bounds, rather than bounds only valid in the vicinity of the origin.

In the limit $\beta \to \infty$ we also expect to be able to tell something about the dynamics since

$$\lim_{\beta \to \infty} \langle \xi \tanh(\beta \xi \mathbf{A} m) \rangle = \frac{1}{2^p} \sum_{\xi = \{\pm 1\}^p} \xi \operatorname{sgn}(\xi \mathbf{A} m)\,. \tag{29}$$

In the continuous-time case this leads to sharp corners in the trajectories, when $\boldsymbol{\xi}\mathbf{A}\boldsymbol{m}$ changes sign. In the discrete-time case, since $\operatorname{sgn}(\boldsymbol{\xi}\mathbf{A}\boldsymbol{m}_t)$ only has two possible values ± 1, and $\boldsymbol{\xi}$ has 2^p possibilities, we expect cycles of maximum period 2^p. However, the sgn function is the limit of a tanh, so there it has a third possible value 0, when $\boldsymbol{\xi}\mathbf{A}\boldsymbol{m}_t = 0$. This admits a further 2^p possibilities, therefore in the limit $\beta \to \infty$ we expect a limit cycle with maximum period 2^{p+1}.

3.2. *One and two patterns*

The dynamics of a network trained with only one pattern (i.e. $p = 1$) is given by one autonomous nonlinear differential, or difference equation

$$\frac{\mathrm{d}m}{\mathrm{d}t} = \tanh(\beta A m) - m \qquad m_{t+1} = \tanh(\beta A m_t)\,. \tag{30}$$

This is a special case of the general equations (1) and (2), for which $\mathbf{A}$ is simply a number, therefore it is necessarily symmetric, and only provides an extra scaling for β. The Lyapunov functions in [17] apply, and the system is guaranteed to reach an equilibrium configuration. Steady-state bifurcations will occur from the trivial fixed points to non-trivial fixed points in the continuous-time case, and to fixed points or period two-cycles (for $A < 0$) in the case of discrete-time dynamics.

A network trained with two patterns (i.e. $p = 2$) is the simplest we expect to display interesting behaviour. It can be analysed directly, since there are a reasonably small number of free parameters, and from these results we hope to infer general statements networks with larger numbers of patterns.

Again we consider the matrix $\mathbf{A} = \begin{pmatrix} 1 & \alpha \\ -\alpha & 1 \end{pmatrix}$ since this is guaranteed to have a complex conjugate pair of eigenvalues, though the extension of the following work to general $\mathbf{A}$ is not difficult. We will only consider the difference equation, since the differential equation cannot display the property of mode locking:

$$\boldsymbol{m}_{t+1} = \frac{1}{2}\begin{pmatrix} 1 \\ 1 \end{pmatrix} \tanh \beta\left[(1-\alpha)m_t^1 + (\alpha+1)m_t^2\right] + \frac{1}{2}\begin{pmatrix} 1 \\ -1 \end{pmatrix} \tanh\left[\beta((\alpha+1)m_t^1 + (\alpha-1)m_t^2\right]. \tag{31}$$

We now change to polar coordinates, the natural coordinate frame in which to consider Hopf bifurcations. Putting $(m^1, m^2) = r(\cos\theta, \sin\theta)$ gives

$$r_{t+1}^2 = \tfrac{1}{2}\tanh^2 a_t r_t + \tfrac{1}{2}\tanh^2 b_t r_t \qquad \theta_{t+1} = \tan^{-1}\left(\frac{\tanh a_t r_t - \tanh b_t r_t}{\tanh a_t r_t + \tanh b_t r_t}\right) \tag{32}$$

with the abbreviations $a_t = \beta((1-\alpha)\cos\theta_t + (\alpha+1)\sin\theta_t)$ and $b_t = \beta((\alpha+1)\cos\theta_t + (\alpha-1)\sin\theta_t)$.

Close to the bifurcation point we expect the radius of the curve to be small, if we expand r_{t+1}^2 in terms of r_t we find

$$r_{t+1}^2 \simeq (a^2 + b^2)r_t^2 - \tfrac{4}{3}(a^4 + b^4)r_t^4 + \mathcal{O}(r_t^6) \tag{33}$$

where $a^2 + b^2$ is independent of θ_t, so angular dependence only enters throught the second, and higher-order terms. As we move away from the bifurcation point, and higher terms need to be taken into account, the angular dependence will become stronger, and higher-order θ_t terms will appear. This will have the effect of making the trajectory more convoluted and less circular as we move away from the bifurcation point, and higher-order angular harmonics become important (figure 2).

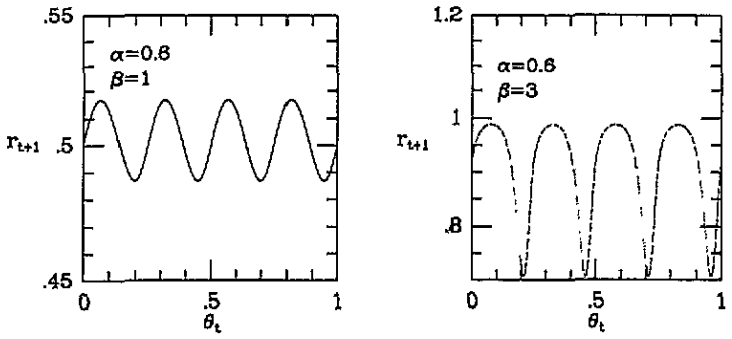

Figure 2. r_{t+1} against θ_t for $\beta = 1$ and $\beta = 3$ showing the increasing angular dependence of r_t as we move away from the bifurcation point.

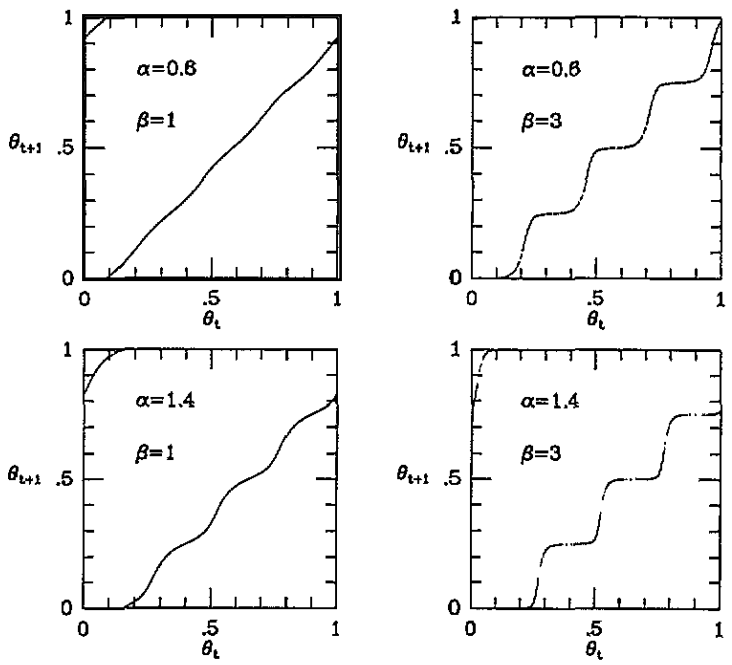

Figure 3. θ_{t+1} against θ_t for $\beta = 1$ and 3, $\alpha = 0.6$ and 1.4 obtained from iterating the dynamics directly. Away from the bifurcation point the maps become stair-like.

If we examine what happens to θ_{t+1} as θ_t is varied, in the limit $\beta \to \infty$, with $\alpha \neq 1$ we see that the tanh functions become sgn functions, so

$$\theta_{t+1} = \tan^{-1}\left(\frac{\mathrm{sgn}((1-\alpha)\cos\theta_t+(1+\alpha)\sin\theta_t)-\mathrm{sgn}((1+\alpha)\cos\theta_t-(-1+\alpha)\sin\theta_t)}{\mathrm{sgn}((1-\alpha)\cos\theta_t+(1+\alpha)\sin\theta_t)+\mathrm{sgn}((1+\alpha)\cos\theta_t-(-1+\alpha)\sin\theta_t)}\right). \tag{34}$$

Hence the function is step like with values $n\pi/2$, changing when $\tan\theta = (\alpha - 1)/(\alpha + 1)$ or $\tan\theta = (\alpha + 1)/(\alpha - 1)$.

Therefore as we increase β from the bifurcation point, we expect the return map of θ_{t+1} against θ_t to go from a straight, diagonal line, to a series of four rounded steps, to a series of four sharp steps (figure 3). As β is increased the points visited by the dynamics tend to

be only at the corners of the steps. At exactly $\beta = \infty$, the function becomes non-invertible. This results in 4-cycles for $\alpha > 1$, fixed points for $\alpha < 1$, and 8-cycles for $\alpha = 1$. At exactly $\beta = \infty$ and $\alpha = 1$, the return map only just touches the diagonal. The behaviour is therefore indeterminate, and depends on the order in which the limts $\beta \to \infty$ and $\alpha \to 0$ are taken.

4. Stability analysis and Arnold tongues

In this section we consider, in detail, the different periodic orbits generated by the nonlinear mappings. If a complex pair of eigenvalues of the linearized equations of motion leading to a Hopf bifurcation are the nth root of unity, then the behaviour close to the trivial fixed point can be considered as a steady-state bifurcation in $m_{t+n} = f(m_t)$. These resonances *cause mode locking. At the bifurcation point, non-resonant eigenvalues form points of zero* measure on the unit circle forming the range of eigenvalues in the complex plane. As we move away from the bifurcation point these points grow, forming Arnold tongues—finite regions in parameter space where the system locks into a given period orbit. As these tongues grow (as some parameter is varied) they may fill all space, leave some space for quasi-periodic orbits or even overlap, causing chaos. These tongues are caused by nonlinear angular terms which become important as we move away from the bifurcation point. This section explores how the tongues grow as parameters are varied in our system, and how the stability of various periodic orbits can be calculated. We use the $p = 2$ system with the matrix $\begin{pmatrix} 1 & \alpha \\ -\alpha & 1 \end{pmatrix}$ as our prototype model, since it has only two parameters to adjust. We present numerical evidence that the $p = 3$ case also displays similar behaviour, however.

Figure 4 shows the winding number (i.e. average rotation per iteration) over a range of β for $0.1 \leqslant \alpha \leqslant 1.9$ in steps of 0.1.

Networks with $\alpha < 1$ tend towards $w = 0$ as β increases and $\alpha > 1$ tend towards $w = 0.25$ as β increases. At exactly $\alpha = 1$, $w = 0.125$ is a stable orbit for all β. Also notice several regions of mode locking where w is an either integer or a rational fraction corresponding to periodic orbits. We can gain much insight into the problem by considering the equations of motion at $\beta = \infty$, then considering how the behaviour will change for

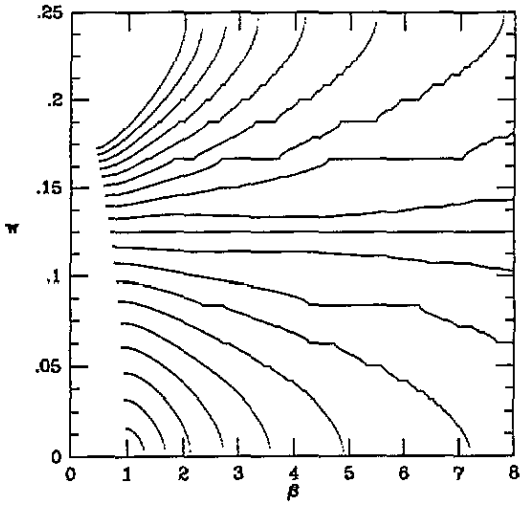

Figure 4. Winding number as a function of β for α from 0.1 at the bottom to 1.9 at the top, in steps of 0.1.

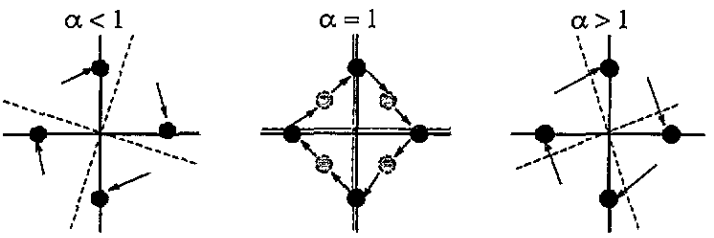

Figure 5. Basin boundaries and trajectories in the m_1–m_2 plane, for $\alpha < 1$, $\alpha = 1$ and $\alpha > 1$. The dotted lines represent the basin boundaries, and the full circles represent points which are visited by the dynamics. The shaded dots represent points on the cycle which only appear when the basin boundaries intersect the axes. The arrows show how points in each region are mapped to points on the cycle.

finite β. For $\beta = \infty$ the tanh functions become sgn functions, and the equations of motion become

$$m_{t+1} = \frac{1}{2}\begin{pmatrix}1\\1\end{pmatrix}\mathrm{sgn}\left((1-\alpha)m_1 + (1+\alpha)m_2\right) + \frac{1}{2}\begin{pmatrix}1\\-1\end{pmatrix}\mathrm{sgn}\left((1+\alpha)m_1 + (-1+\alpha)m_2\right) . \tag{35}$$

Since the mapping now contains sgn functions, any point within a certain boundary will be mapped to a single point. Basin boundaries are given by $m_1/m_2 = (\alpha+1)/(\alpha-1)$ and $m_1/m_2 = (1-\alpha)/(1+\alpha)$. The behaviour of points exactly on a boundary is marginal, they will first be mapped into a basin, and then onto an appropriate point.

We can investigate the behaviour by considering what happens to the basin boundaries as α is varied, as depicted in figure 5. Starting at $\alpha = 0$ the basin boundaries are the diagonals $m_1 = \pm m_2$. Consider the upper quadrant, here all points are mapped to (0, 1), hence there are four equivalent fixed points, since all points within each quadrant are mapped to a point within that quadrant. As α is increased the boundary lines rotate anti-clockwise. At $\alpha = 1$ the basin boundaries intersect the axis, and hence also the fixed points. Here the behaviour changes, since the points to which the dynamics maps are on the boundaries and hence the behaviours are marginal. The points on the axis will, in fact, be mapped clockwise to the points $\left(\pm\frac{1}{2}, \pm\frac{1}{2}\right)$. The trajectory is now in another basin, and will again be mapped clockwise to a point on the next axis. Hence an 8-cycle is established. For $\beta = \infty$ this only occurs for $\alpha = 1$. As α is increased further past 1, the boundaries continue to rotate anti-clockwise, once they have passed the axes, however, the points mapped to are no longer in the same quadrant, therefore a 4-cycle results.

As β is decreased the points visited by the dynamics deviate slightly from the axes. Behaviour need not be restricted to fixed points, 4-cycles and 8-cycles, but also a wealth of integer-period cycles and quasi-periodic cycles may appear. The basin boundaries now become meaningless, and the type of behaviour must be determined by a stability analysis, using the Jacobian of the mapping $\left(\partial m_{t+1}^{\alpha}/\partial m_t^{\beta}\right)$. If we consider some finite value of β and increase α from zero, we go from fixed points through quasi-periodic and other period cycles, to an 8-cycle, then through another region of quasi-periodic and periodic cycles, to a 4-cycle.

For $\alpha = 1-\epsilon$, the fixed points are of the form $(1-\delta, \mathrm{sgn}(\epsilon)\delta)$ and its analogues close

to the other axes, for large β, where δ is a function of ϵ and β. As β increases δ decreases to zero. For ϵ close to zero, there are not only points close to the axes visited by the dynamics, but also points in between. For moderate β these are close to $(\pm\frac{1}{2}, \pm\frac{1}{2})$, but as β is increased these become closer to the axes, so that points visited by the dynamics are like $(1-\delta_1, \delta_1)$ and $(1-\delta_2, -\delta_2)$. δ_1 and δ_2 decrease as β is increased, and at $\beta = \infty$ these two points merge on the axis, and other points are created at $(\pm\frac{1}{2}, \pm\frac{1}{2})$.

We commence the stability analysis by calculating the Jacobian of the mapping using (31). In principle from this we can calculate the critical stability line of any cycle in β–ϵ-space. In general though, this is difficult, apart from certain cycles for which symmetries simplify the problem.

4.1. Fixed points, 4-cycles and 8-cycles

First we consider the case of $\alpha = 1 - \epsilon$ giving rise to fixed points. Since all fixed points are equivalent, we take the one near $(1, 0)$, and use the postulated form $(1 - \delta + \mathcal{O}(\delta^2), -\delta + \mathcal{O}(\delta^2))$, this implies that $\tanh\beta((2-\epsilon)m_1 - \epsilon m_2) \simeq 1 + \mathcal{O}(\delta^2)$ and $\tanh\beta(\epsilon m_1 + (2-\epsilon)m_2) \simeq 1 - 2\delta + \mathcal{O}(\delta^2)$. Using these results and keeping only linear terms in δ the Jacobian becomes $2\beta\delta\begin{pmatrix}\epsilon & 2-\epsilon\\ \epsilon & 2-\epsilon\end{pmatrix}$. This assumes that β is large so that $\delta \ll 1$. Now critical stability occurs when the maximum absolute value of any eigenvalue of the Jacobian is 1, which is given by $4\beta\delta = 1$. In order to obtain a value for δ in terms of β and ϵ only expand $\tanh\beta(\epsilon m_1 + (2-\epsilon)m_2)$ around the fixed point $(1-\delta, -\delta)$, assuming $\delta < \epsilon$, and that $\beta\epsilon$ is large giving

$$\delta \simeq \frac{1 - \tanh\beta\epsilon}{2\big(1 - \beta\big(1 - \tanh^2\beta\epsilon\big)\big)}. \tag{36}$$

Since the numerator is neccesarily positive, and δ is positive, a restriction is placed on the range of β and ϵ for which this expression is valid: $\epsilon > 1/\beta\tanh^{-1}(1 - 1/\beta)$, as well as the condition for the expansion to be valid $\beta\delta \ll 1$, $\delta < \epsilon$, and $\beta\epsilon \gg 1$. Hence

$$\frac{2\beta(1 - \tanh\beta\epsilon)}{\big(1 - \beta\big(1 - \tanh^2\beta\epsilon\big)\big)} - 1 = 0 \tag{37}$$

defines a relationship between β and ϵ, valid in the high-β limit giving the stability boundary of the fixed point. This equation must be solved numerically.

If we let β go to infinity along the line defined by (37) we can determine the asymptotic form of the line defining the stability in this limit. Writing $\tanh x \simeq 1 - 2e^{-2x}$ for $x \to \infty$ this gives an equation $8\beta e^{-2\beta\epsilon} - 4\beta e^{-4\beta\epsilon} = 1$. Assuming that $e^{-4\beta\epsilon}$ is negligible compared with $e^{-2\beta\epsilon}$ this gives a form like $\epsilon \sim (\log 8\beta)/2\beta$, so $\alpha \sim 1 - (\log 8\beta)/2\beta$.

A similar relationship can be derived for the 4-cycle, with $\alpha = 1 + \epsilon$, using similar arguments and the relations between succesive points on the cycle. Since all points on the 4-cycle are equivalent the Jacobian need only be calculated at one point. The Jacobian at $(-\delta, 1-\delta)$ is $2\beta\delta\begin{pmatrix}2+\epsilon & \epsilon\\ -2-\epsilon & -\epsilon\end{pmatrix}$, with critical stability again given by $4\beta\delta = 1$. In order to calculate δ we expand the mapping at the transition $(-\delta, 1-\delta) \to (1-\delta, \delta)$ giving

$$\delta = \frac{1 - \tanh\beta\epsilon}{2\big(1 - \beta(\epsilon+1)\big(1 - \tanh^2\beta\epsilon\big)\big)} \tag{38}$$

where again we have assumed $\beta\delta \ll 1$, $\delta < \epsilon$ and $\beta\epsilon \gg 1$. The equation governing the stability for the 4-cycle, for large β is then

$$\frac{2\beta(1 - \tanh\beta\epsilon)}{\big(1 - \beta(\epsilon+1)\big(1 - \tanh^2\beta\epsilon\big)\big)} - 1 = 0. \tag{39}$$

We can derive the asymptotic functional form, in the same way as for the fixed points: $\epsilon \sim (\log 4\beta(2+\epsilon))/2\beta$, so $\alpha \sim 1 + (\log 8\beta)/2\beta$.

We can calculate the stability line for the 8-cycle in a similar way, though in this case it is slightly more complex, since the 8-cycle contains two set of non-equivalent points, hence two Jacobians and two δ's must be calculated.

First we take the case $\alpha = 1 + \epsilon$, we consider the $(1-\delta_1, -\delta) \to (\delta_2, -1+\delta_2) \to (-\delta_1, -1+\delta_1)$ part of the trajectory. The Jacobians at the first two points are

$$\begin{aligned} J^+(1-\delta_1, -\delta_1) &= 2\beta\delta_2 \begin{pmatrix} -\epsilon & 2+\epsilon \\ -\epsilon & 2+\epsilon \end{pmatrix} + \mathcal{O}(\delta_2^2) \\ J^+(\delta_2, -1+\delta_2) &= 2\beta\delta_1 \begin{pmatrix} 2+\epsilon & \epsilon \\ -2-\epsilon & -\epsilon \end{pmatrix} + \mathcal{O}(\delta_1^2)\,. \end{aligned} \tag{40}$$

The critical stability line is therefore given by the eigenvalue of their product with the largest magnitude: $16\beta^2\delta_1\delta_2(\epsilon+1)^2 = 1$. We calculate δ_1 and δ_2 as before by expanding the dynamic equations, with $\delta_1\beta \ll 1$ though in contrast to before $\delta_2 > \epsilon$, and $\epsilon > \delta_1$. The equations for δ_1 and δ_2 are then

$$\delta_1 = \mathrm{e}^{-2\beta(2\delta_2-\epsilon)}\delta_2 = \tfrac{1}{2}(1-\tanh\beta\epsilon) + \beta\delta_1\big(1-\tanh^2\beta\epsilon\big)\,. \tag{41}$$

From the equations for δ_1 and δ_2 and the critical stability relation it is possible to derive an equation involving β and ϵ only, determining the critical stability of the 8-cycle for $\alpha > 1$ and large β.

If we use the critical stability equation to create a quadratic form for δ_2, we can again determine the asymptotic limit for the line, and find $\epsilon \sim (\log 2\beta)/\beta - (\log\log 16\beta^2)/\beta$ so $\alpha \sim 1 + (\log 2\beta)/\beta - (\log\log 16\beta^2)/\beta$.

Similarly for $\alpha = 1-\epsilon$ we study the $(1-\delta_1, \delta_1) \to (1-\delta_2, -\delta_2) \to (\delta_1, -1+\delta_1)$ part of the trajectory. The Jacobians at the first two points are

$$\begin{aligned} J^-(1-\delta_1, \delta_1) &= 2\beta\delta_2 \begin{pmatrix} \epsilon & 2-\epsilon \\ \epsilon & 2-\epsilon \end{pmatrix} + \mathcal{O}(\delta_2^2) \\ J^-(1+-\delta_2, -\delta_2) &= 2\beta\delta_1 \begin{pmatrix} \epsilon & 2-\epsilon \\ \epsilon & 2-\epsilon \end{pmatrix} + \mathcal{O}(\delta_1^2)\,. \end{aligned} \tag{42}$$

The critical stability line is now given by $16\beta^2\delta_1\delta_2 = 1$. In order to calculate δ_1 and δ_2 we again assume that $\beta\delta_1 \ll 1$ and $\delta_2 > \epsilon$, giving the following expressions:

$$\delta_1 = \mathrm{e}^{-2\beta(2\delta_2-\epsilon)} \qquad \delta_2 = \tfrac{1}{2}(1-\tanh\beta\epsilon) + \beta\delta_1(\epsilon-1)\big(1-\tanh^2\beta\epsilon\big)\,. \tag{43}$$

These again form a set of equations to be solved numerically giving the critical stability of the 8-cycle region for large β.

Again the asymptotic form of the solution can be found: $\epsilon \sim (\log 4\beta)/2\beta - (\log\log 16\beta^2)/2\beta$ and $\alpha \sim 1 - (\log 4\beta)/2\beta + (\log\log 16\beta^2)/2\beta$.

4.2. Mode-locked regions

Using this information we can construct a phase diagram for the network, showing the boundaries of stability of the different period cycles. The natural coordinates to use are T/T_c and $1/T_c$, where $T = 1/\beta$ and $T_c = \sqrt{1+\alpha^2}$ is the temperature at which the system bifurcates from the trivial fixed point. Figure 6 shows the phase diagram, with the dots calculated from the above stability analysis, and the lines taken between critical stability points from iterations of the mappings directly. The markers are from calculations of the asymptotic form.

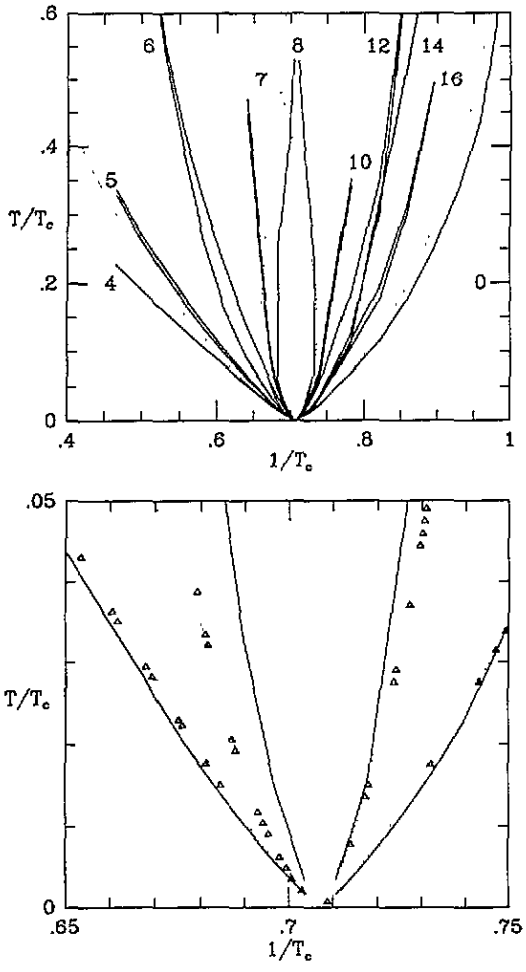

Figure 6. *Phase diagram showing the different periodic trajectories. The number represents the period in the particular region. The dots mark points calculated from the preceding stability analysis; the triangles are points taken from the $\beta \to \infty$ asymptotic form of these equations; and the straight lines join points taken from direct iteration of the dynamic equations. The lines are meant as a guide between points only. Only a restricted number of periodic regions is shown in order not to crowd the diagram.*

The fit is only qualitative for moderate T, however, for small T ($\beta \to \infty$) all three sets of data converge. In between the regions shown on the diagram are other regions corresponding to periodic orbits, which have not been shown in order that the diagram be comprehensible. In between these mode-locked regions are regions of quasi-periodicity, which shrink as $T \to 0$.

We expect similar behaviour to occur in networks trained with any number of patterns, since the normal forms are the same up to cubic order. Figure 7 shows the winding number and 1/period for a network trained with three patterns, using the matrix (23), with an arbitary linear combination ($m_1 + m_2$ and m_3) as the two coordinates. The winding number shows similar behaviour to the $p = 2$ case with many mode-locked steps, showing that a Hopf bifurcation leads to motion with only two free variables. The period is measured to be the number of steps required to return arbitarily close to the starting point. We see that in the mode-locked steps the winding number and 1/period are the same. This is as we would expect. Out of the mode-locked regions, i.e. in the quasi-periodic regime, the period is higher than the winding number would suggets, reflecting the fact that the period must be integer.

In principle, we could construct a phase diagram for networks with arbitary matrix **A**.

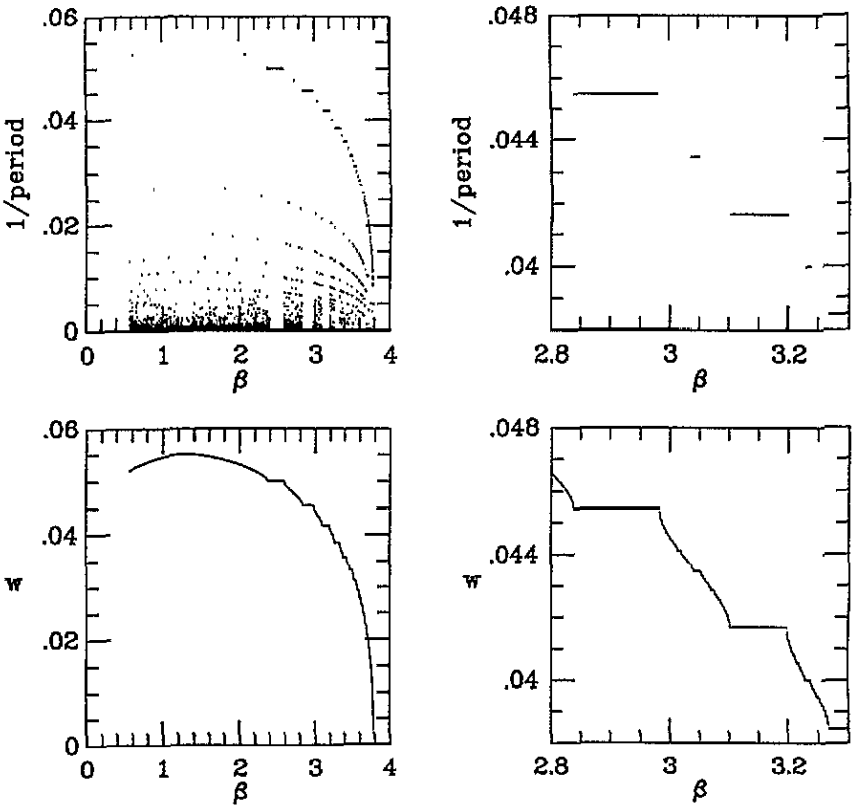

Figure 7. Winding number and 1/period for $p = 3$.

Since there are p^2 free parameters the phase diagram would need to be in p^2-dimensional space. As we varied any one of the parameters, keeping β (the overall scaling factor) fixed, we would go through a range of periodic and quasi-periodic orbits. The precise shape of the various regions would depend on the numerical values in the embedding matrix **A**. There would, however, be certain regions which we can readily identify.

(i) The fixed-point region corresponding to symmetry of **A** when all eigenvalues are pure real.

(ii) The 4-cycle region corresponding to complete asymmetry of **A** when all eigenvalues are pure imaginary.

(iii) The 2^{p+1}-cycle region which for $\beta = \infty$ corresponds to the basin boundaries coinciding with the axes.

5. Conclusion

In this paper we have studied the qualitative behaviour of stochastic Ising spin neural networks, with separable interactions. The macroscopic variables (pattern overlaps) which in the limit $p \ll \sqrt{N}$, $N \to \infty$ (where p is the number of patterns and N is the number of neurons) evolve due to the deterministic laws (1) and (2) for asynchronous and synchronous updating of the neurons, respectively, show a variety of bifurcation phenomena if the noise (parametrized by an inverse temperature, β) and the eigenvalues of the embedding matrix **A**

are varied. We have shown that the qualitative behaviour of such types of neural networks can be analysed using the methods of bifurcation theory. These methods can be used to predict when and how the system will move away from the trivial fixed point and we have shown that the type of bifurcation is dependent only on the form of the eigenvalue of **A** with the largest real part (in the continuous-time case) or the largest modulus (in the discrete-time case). Away from the critical point non-trivial and quasi-periodic cycles appear, due to the nonlinear angular terms becoming important. These are the *Arnold tongues*, and the stability of these cycles can be calculated in the large-β limit. Hence a phase diagram may be constructed in the p^2 dimensions of the free parameters of the embedding matrix **A**. This phase diagram shows how the regions where different periodic orbits are stable are affected by changes to the elements in **A**. In between the mode-locked periodic phases are regions of quasi-periodic behaviour where the period of the orbit is irrational, hence the system returns close to its starting point, but never coincides with it.

We have supported our analysis with numerical simulations which illustrate the types of behaviour encountered. In this way we have shown the condition neccesary for a recursive neural network of this separable type to show the properties of

(i) associative memory is $\lambda^* \in \mathbb{R}$;
(ii) sequence retrieval is $\lambda^* \in \mathbb{R} + \mathbb{I}$

where λ^* is the eigenvalue of **A** with the largest real part in the continuous-time case, or the largest modulus in the discrete-time case. We have shown that in the case of sequence retrieval the period depends both on the eigenvalues of the embedding matrix **A** and the noise, parametrized by β. Hence for a network with a given amount of internal noise the eigenvalues of the embedding matrix **A** must be tuned in order to be able to retrieve a given sequence.

Acknowledgment

We acknowledge financial support from the EPSRC under grant numbers 92310910 and GRH73028.

References

[1] Coolen A C C and Ruijgrok T W 1988 *Phys. Rev.* A **38** 4253
[2] Riedel U, Kühn R and van Hemmen J L 1988 *Phys. Rev.* A **38** 1105
[3] Bernier O 1991 *Europhys. Lett.* **16** 531
[4] Coolen A C C and Sherrington D 1993 *Mathematical Approaches to Neural Networks* ed J G Taylor (Amsterdam: North-Holland) ch 9 p 293
[5] Coolen A C C and Sherrington D 1993 *Phys. Rev. Lett* **71** 3886
[6] Sompolinsky H, Crisanti A and Sommers H J 1988 *Phys. Rev. Lett* **61** 259
[7] Bauer M and Martienssen W 1989 *Europhys. Lett.* **10** 427
[8] Aihara K, Takabe T and Toyoda M 1990 *Phys. Lett.* **144A** 333
[9] Bauer M and Martienssen W 1991 *J. Phys. A: Math. Gen.* **24** 4557
[10] Tirozzi B and Tsodyks M 1991 *Europhys. Lett.* **14** 727
[11] Wang L and Ross J 1991 *Phys. Rev.* A **44** R2259
[12] Bollé D, Shim G M, Vinck B and Zagrebnov V A 1994 *J. Stat. Phys.* **74** 565
[13] Bollé D, Shim G M and Vinck B 1994 *J. Stat. Phys.* **74** 583
[14] Crisanti A, Falcioni M and Vulpiani A 1993 *J. Phys. A: Math. Gen.* **26** 3441
[15] Nutzel K 1991 *J. Phys. A: Math. Gen.* **24** L151
[16] Peretto P 1984 *Biol. Cybern.* **50** 51
[17] Laughton S N and Coolen A C C 1994 *Preprint* OUTP-94-205 (submitted to *J. Stat. Phys.*)
[18] Crawford J D 1991 *Rev. Mod. Phys.* **63** 991
[19] Khalil H K 1992 *Nonlinear Systems* (New York: Macmillan)
[20] Arnold V I 1978 *Ordinary Differential Equations* (Berlin: Springer)

[21] Rasband N S 1990 *Chaotic Dynamics of Nonlinear Systems* (New York: Wiley)
[22] Hartman P 1982 *Ordinary Differential Equations* (Boston: Birkhäuser)
[23] Feigenbaum M J 1977 *J. Stat. Phys.* **19** 25
[24] Feigenbaum M J 1979 *J. Stat. Phys.* **21** 669
[25] Coolen A C C and Sherrington D 1992 *J. Phys. A: Math. Gen.* **25** 5493